

A New Generation of Mid-Infrared Sensors Based on Quantum Cascade Laser

Dibyendu Dey, John Kohoutek, Ryan. M. Gelfand, Alireza Bonakder, and Hooman Mohseni¹

Department of Electrical Engineering and Computer Science

Bio-Inspired Sensors and Optoelectronics Laboratory (BISOL)

Northwestern University, Evanston, IL 60208, USA

ABSTRACT

Many important bio and chemical molecules have their signature frequency (vibrational resonance) matching the mid infrared region (2-10 μm) of the optical spectrum. But building a bio-sensor, sensitive in this spectral regime, is extremely challenging task. It is because of the weak light-particle interaction strength due to huge dimensional mismatch between the probed molecules (typically ~ 10 's of nm) and the probing wavelength (order of micron). We exploit the optical antenna to overcome this problem by squeezing the optical modes. This modal confinement happens only in the near-field region of the antenna and thus we have built an apertureless near-field scanning optical microscope (a-NSOM) to demonstrate it experimentally. Further, we have integrated these plasmonic antennas with mid-infrared sources known as Quantum Cascade Lasers (QCL). Our antenna structure is based on metal-dielectric-metal (MDM) and we have shown how they can generate higher electrical field enhancement compared to single metal design. Antenna integrated QCL operated at room temperature and its wavelength of operation was measured to be $\sim 6\mu\text{m}$. We have used 3D finite-difference-time-domain (FDTD) simulations to optimize the different component of the MDM antenna. After optimizing, we fabricated the antenna on the facet of QCL using focused ion beam (FIB) and measured using a-NSOM. We have shown that the optical mode can be squeezed down to a few 100 's of nm which is much smaller than the incident light wavelength ($\lambda \sim 6\mu\text{m}$). We also propose a microfluidic approach to build a typical mid-infrared bio-sensor where the probed molecules can be transferred to the near field region of the antenna through fluidic channels. Such scheme of building bio-sensor can overcome the barrier of weak light-particle interaction and eventually could lead to building very efficient, compact, mid-infrared bio-sensors.

Key words: Bio-sensing, Focused ion beam milling, Field enhancement, Micro-fluidics, Near-field imaging, Optical antenna, Plasmonics, Quantum Cascade Laser, Surface plasmon resonance.

¹ hmohseni@ece.northwestern.edu, www.bisol.northwestern.edu

1. INTRODUCTION

Surface plasmons (SP)¹ is a collective oscillation of charges at the interface between metal and dielectric. Such surface wave has long propagation length and avoids the metal loss (as most of the part of the surface wave stays in dielectric). SP wave can be generated using an incident light beam with satisfying the fundamental law of conservation of momentum. The principle of surface plasmons has been extensively applied in many novel applications for example extraordinary optical transmission^{2,3,4}, label-free measurements of bio-molecular sensing^{5,6}, drug discovery^{7,8}, surface plasmon interference lithography⁹ and spectroscopic applications¹⁰. By solving the Maxwell's equation in a planar film, the SP dispersion relationship is found to be:

$$k = \frac{\omega}{c} \sqrt{\epsilon_{eff}} \quad (1)$$

Where, k is the wave vector of the electromagnetic field propagation parallel to the interface between metal and dielectric, ω is the angular frequency of the incident field. ϵ_{eff} is the effective dielectric constant given by:

$$\epsilon_{eff} = \frac{\epsilon_d \epsilon_m}{\epsilon_d + \epsilon_m} \quad (2)$$

Where, ϵ_m and ϵ_d represent the dielectric constants for metal and dielectric respectively. As formula (1) suggests, the angular momentum of SP is greater than the free space momentum of incident photon and thus exciting SP at the metal-dielectric interface requires special technique to compensate the difference in momentum. Previously, it has been achieved using two different coupling techniques – prism coupler¹ or grating coupler¹¹.

Although the fundamental principle remains unchanged, generation of SPs in microscopic object like nanoparticles require more rigorous optical theories and Mie theory¹² has addressed the solution of Maxwell equation with full complexity for such light-particle interaction. Mie theory suggests that a collective charge oscillation i.e. SP gets induced when an incident electromagnetic field interacts with the target nano particle. Moreover the oscillating frequency matches with the frequency of incident field. For such small particle size, SP is dipolar¹³. It induces the charge accumulation process at the two ends of the nano particle with opposite polarity. The accumulated charge generates strong electric field in the near field region of the nano particle due to coulomb interaction. Such phenomena expand the realm of geometric optics to focus radiant visible and infrared light down to nanometric length scale much smaller compared to its wavelength.

In the past decade, there has been considerable amount of research on optical antennas due to its novel photonic application including chemical^{14,15} and thermal sensors^{16,17}, near-field microscopy^{18,19}, nanoscale photodetectors²⁰ and plasmonic devices^{21,22,23}. Like RF antenna, optical antennas are resonant structures responding to specific wavelengths through both the geometrical and material characteristics of the antenna as well as the surrounding environments^{24,25,26}. Though both optical and RF have fundamental application in controlling radiation pattern, there do exist some basic differences. For example, radio frequency (RF) antenna designs²⁷ wholly focus on optimization of far-field characteristics in order to obtain better long distance transmission and reception performance. In contrast optical antenna emphasize on the near field behavior because the enhancement decays rapidly with distance. Further, the primary challenge of dimensional mismatch between the wavelength and the emitter/receiver (e.g. molecules) for optical antenna is met by improvement in near-field coupling instead of using a feed line as in the RF case.

Significant works related to optical antenna in visible spectrum²⁸ has been previously demonstrated. Recently there has been an added interests in infrared (IR) optical antenna due to relatively ease of structural fabrication compared to visible range, and more importantly the great technological need for its potential applications in chemical spectroscopy, remote sensing, ultrafast IR and THz transient detection^{29,30}. Many of the demonstrated infrared optical antennas were designed based on an external IR laser source^{31,32,33}. Integration of optical antenna along with an IR source was far-reach for a long time due to the absence of any efficient laser source in this optical regime (2-10 μm) till the field of Quantum Cascade Laser matured significantly in the last decade. Since its first demonstration³⁴ in 1994, QCL – a unipolar semiconductor laser³⁵ which works on the principle of intersubband transitions, showed watt level power performance at room temperature³⁶. Group lead by Fredrico Capasso at Harvard University, first demonstrated a fully integrated mid-infrared optical antenna based on QCL and showed a strong near field localization^{37,38,39,40,41,42}. Such optical antenna showed great promise in microscopic application below diffraction limit. The usefulness can be extended further to chemical and bio sensing application if composite material (multilayered) is used instead of single metal as optical antenna element as it paves the way to functionalize different layers.

Here, we demonstrate a metal-dielectric-metal (MDM) based antenna design, where surface plasmon waves at two metal interfaces get coupled by the sandwiched dielectric medium. In comparison to a metal nanorod antenna, such a design promises stronger light enhancement. Furthermore, as a result of higher number of geometrical singularities or sharp edges present in the MDM structure, it can increase the number of regions with local hot spots making it extremely useful for bio-sensing applications^{43,44}. Moreover the design is superior to a single metal nanorod because it opens up the possibility of use it for many bio-sensing applications where different probe molecules can be attached to different layers of the same nanorod⁴⁵.

2. SIMULATIONS

To analyze the performance of our MDM antenna compared to metal nanorod antenna, we first simulated the structure using commercially available 3d FDTD software, Lumerical. All material data used in the simulation, other than the laser region, is from ref 46. The refractive index of the laser material is chosen to be 3.2, which is the weighted average of the refractive index of the active region, $\text{In}_{0.44}\text{Al}_{0.56}\text{As}/\text{In}_{0.6}\text{Ga}_{0.4}\text{As}$. The simulated structure has a 100nm buffer silicon dioxide followed by the metal-dielectric-metal antenna. A schematic diagram of the simulated structure is shown in the inset of Figure 1. An optical TM polarized plane wave with central wavelength around 5.97 μm and it is used as the source for all performed FDTD simulations.

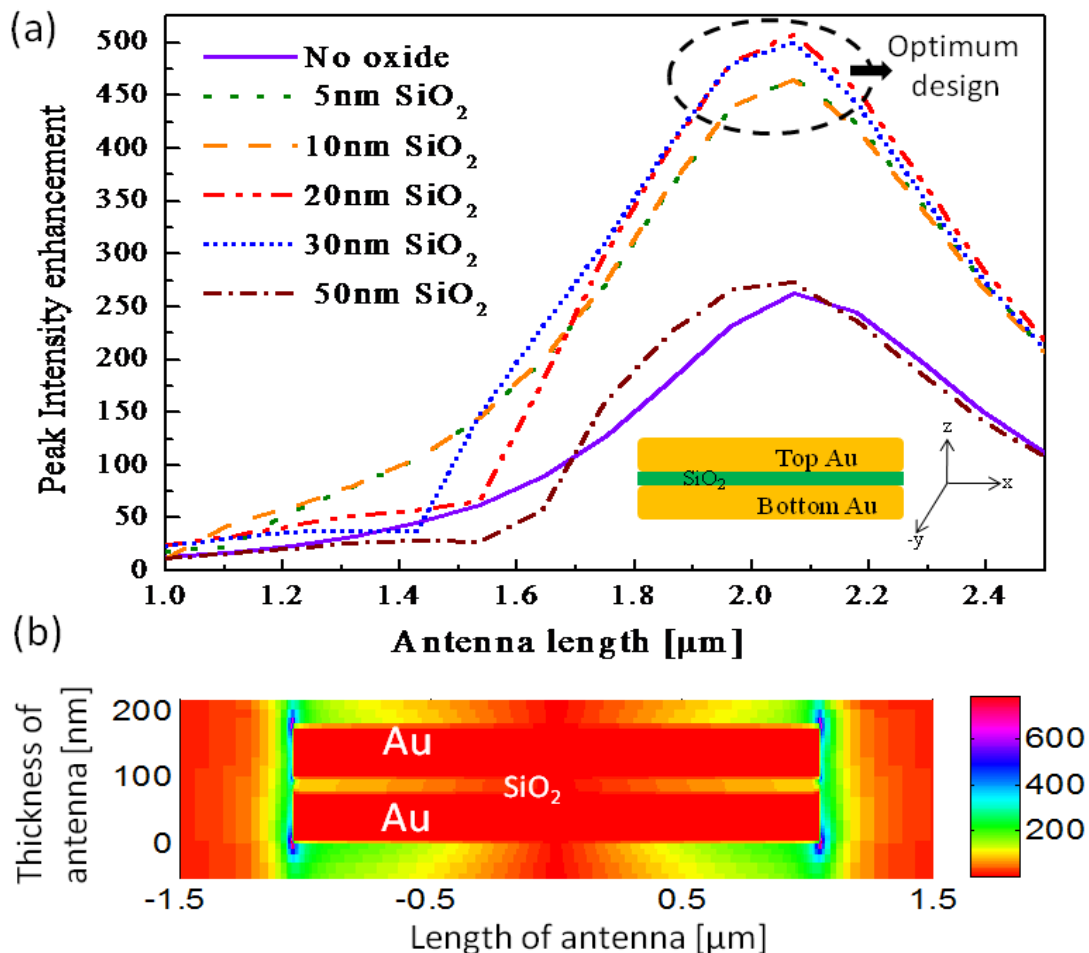


Figure 1 - (Color online) FDTD simulation shows the peak intensity enhancement vs antenna length at $\lambda=5.98 \mu\text{m}$. The silicon dioxide thickness for MDM structure has been varied from 0, 5, 10, 20, 30 to 50 nm,

while keeping the total thickness of the structure to be constant at 170nm. Inset: schematic diagram of the MDM single nanorod. (b) Simulated E-field intensity distribution of the $y=0$ plane for MDM nanorod (Au-SiO₂-Au) at a resonant length of 2.0 μm . It also shows the location of multiple hot spots with high peak intensity ~ 500 times the incident field intensity.

At resonance, surface charge is accumulated at the end of each nanorod and it is maximized at the gap between two closely placed nanorods due to capacitive coupling. The accumulated charge leads to large electric field intensity enhancement at its vicinity. Peak electric field enhancement is plotted against varying lengths of the nanorod antenna (Figure 1). In the simulations, we varied the SiO₂ thickness from 0, 5, 10, 20, 30 to 50 nm, while keeping the total structure thickness to be 170nm. It can be seen that by increasing the SiO₂ thickness from 5 to 10nm, the average intensity is enhanced. It is maximized at a thickness of 20nm and decreases at an oxide thickness of 30nm⁴⁷. We also performed identical simulations for MDM coupled nanorod antenna⁴⁸ and the results have shown in Figure -2.

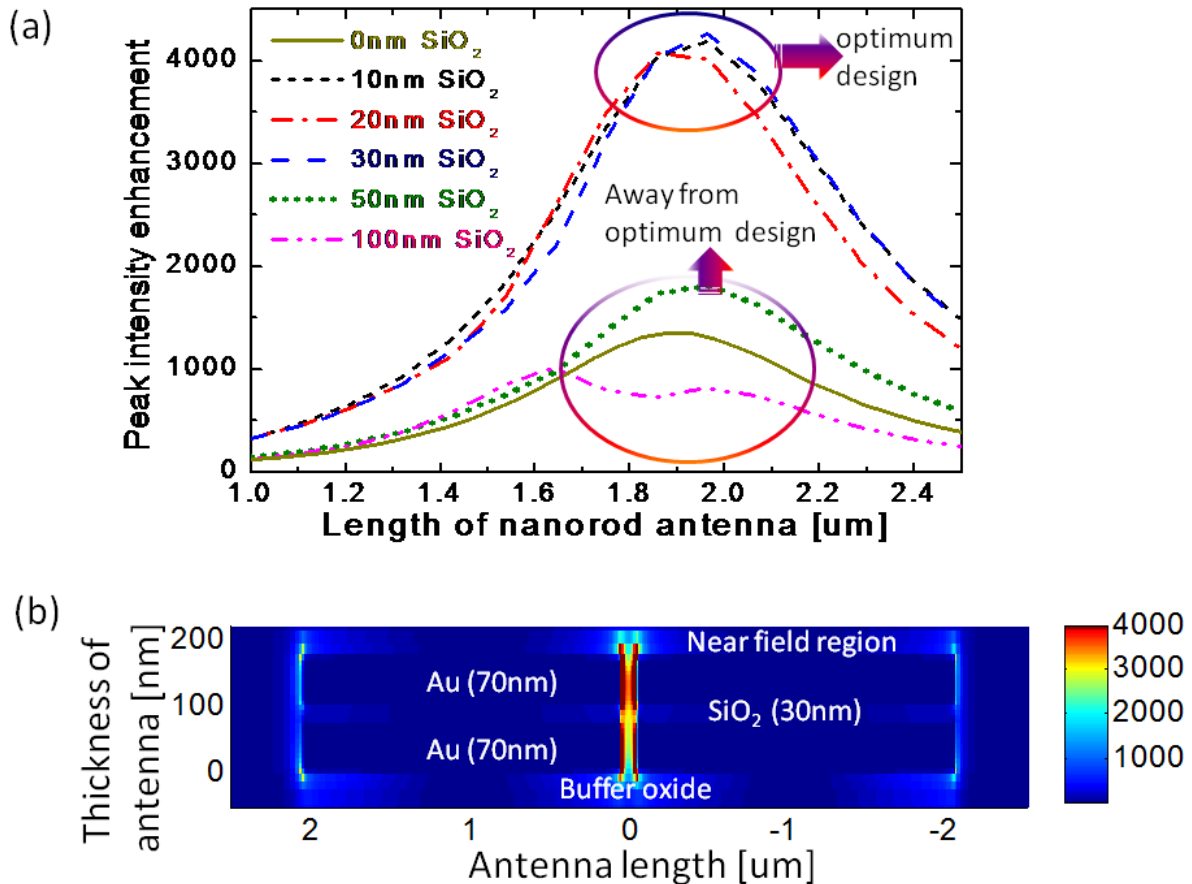


Figure 2 - (a) Plot shows the peak intensity enhancement vs antenna length. The silicon dioxide thickness for MDM structure has been varied from 0, 10, 20, 30, 50 and 100nm, while keeping the total thickness of the structure to be constant at 170nm. **(b)** Side view of the simulated intensity profile for MDM antenna (Au/SiO₂/Au; 70-30-70 nm) at resonance antenna length of 2 μm .

The physics of metal-dielectric-metal antenna is substantially different compared to a single metal design. In short, MDM design works based on a multiple-coupling mechanism. If viewed in time domain, the incident laser light first generates surface plasmons on the bottom Au/buffer SiO₂ interface. Due to vertical plasmon coupling, surface charges are induced on the top Au. Finally, the induced dipole moments at each vertically coupled Au antennas couple radiatively to generate strong near field enhancement. This could also be viewed in frequency domain (steady state) using coupled mode theory, which has been covered extensively in the literature.

3. FABRICATION

The nanorod antenna was then fabricated on the coated facet of the laser using a Focused Ion beam (Hellios FEI). The laser facet was first coated with a buffer insulating oxide followed by the metal-dielectric-metal (Au/SiO₂/Au) layers. We experimented with different oxides like silicon dioxide, magnesium oxide for fabricating devices. Using the gallium ion beam at high voltage (30keV) and low current (48pA), a high precision of milling was achieved. The fabricated antenna on the facet of QCL is shown in the inset of Figure 2(a) and Figure 2 (b) shows a magnified SEM image of the coupled antenna. The threshold current of the laser at room temperature, operating in pulsed mode with 1% duty cycle (100ns, 100 KHz), was found to be 2.28A and 1.68A respectively with and without fabricated antenna. The reduction in threshold current is due to increasing reflectivity from the facet by the metal coating.

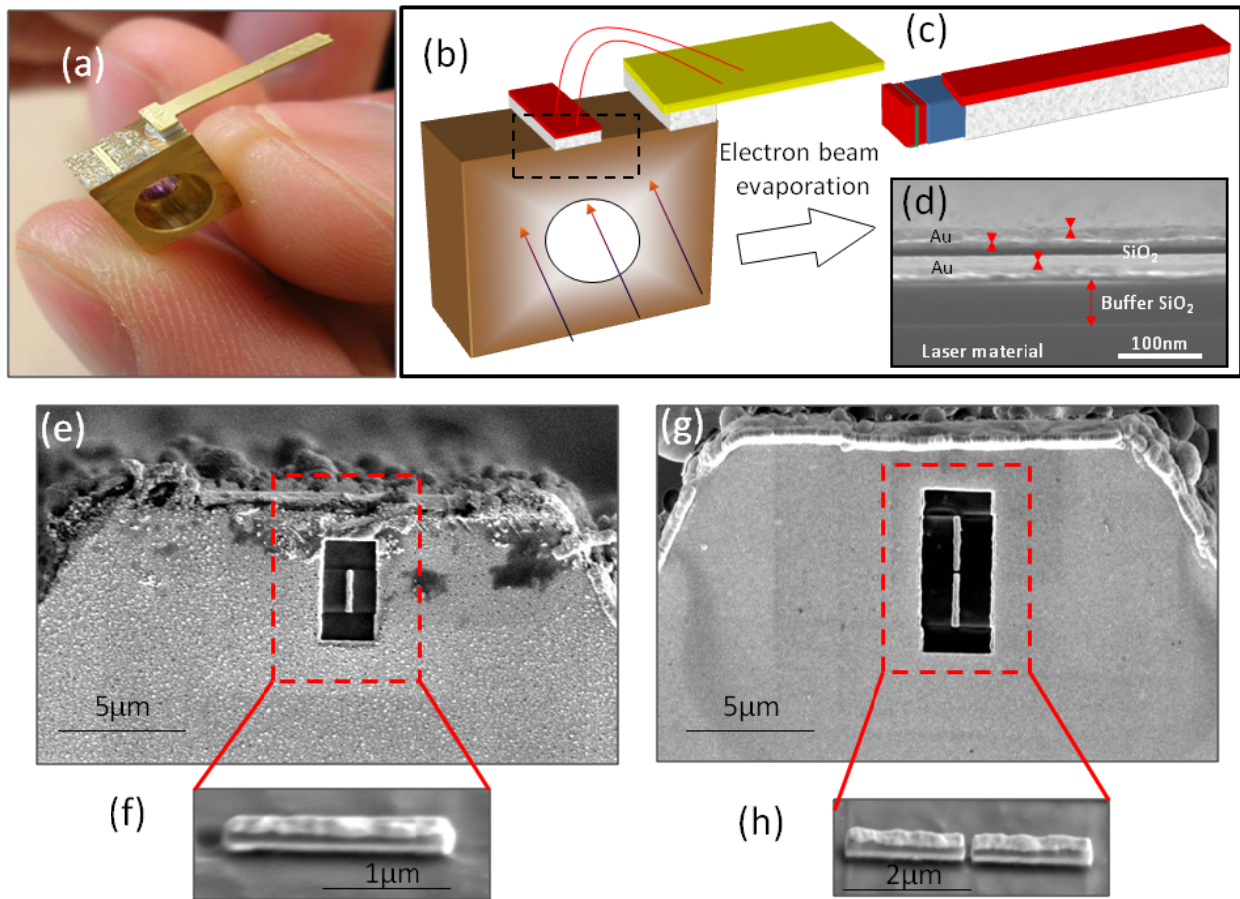


Figure 3 – (a) Image of a packaged Quantum Cascade Laser. (b) Schematic diagram showing the mounted laser and its facet before any coating. (c) Schematic diagram of the coated facet of the QCL. (d) SEM image of the cross-section of MDM antenna showing different layers of the evaporated materials. (e) SEM image of the QCL facet with fabricated MDM single nanorod antenna. A cross-sectional view of the nanorod is shown in (f). (g) SEM image of the MDM coupled nanorod antenna fabricated on the QCL facet and the cross-sectional view is shown in (h).

4. EXPERIMENTAL SET-UP

We used apertureless near-field scanning optical microscope (a-NSOM) to study the near-field of the antenna integrated QCL⁴⁹. A-NSOM offers spatial resolution up to few tens of nanometers and independent of any wavelength. The experimental set-up has been illustrated in Figure -4. The tip of an atomic force microscope (AFM) scans parallel to the surface normal of the antenna in tapping mode. Local electromagnetic field from the antenna structure is scattered by the AFM tip. Part of it gets transmitted through the laser cavity and collected by a mercury-cadmium telluride (MCT) detector after beam collimation. The scattered signal possesses local field information. However, there is also scattering from the cantilever which produces a huge background noise. This background has been overcome by modulating the distance between the probe and the sample. At a small distance between the probe and sample, the apex signal gets hugely enhanced. There is also a contribution to the modulated signal from many other scattering centers along the probe shaft. But the signal contribution of the more distant ones can be effectively suppressed due to their rapid fading at larger distance from the sample^{50,51}. Thus modulating the signal using AFM in tapping mode and then demodulating using a lock-in amplifier can give an excellent background suppressed near-field signal.

Due to selection rule for intersubband transition, QCL emits TM polarized light⁵², where direction of the electric field is along the growth direction. The antenna structure is integrated on the facet of the QCL such that the antenna axis coincides with the direction of laser polarization. Such condition makes the antenna resonant with the incident laser frequency and enhances the near field. There is also a perturbation effect on the antenna near-field due to the presence of probing tip, but it can be suppressed by using dielectric tip instead of metal tip as been suggested in ref 53.

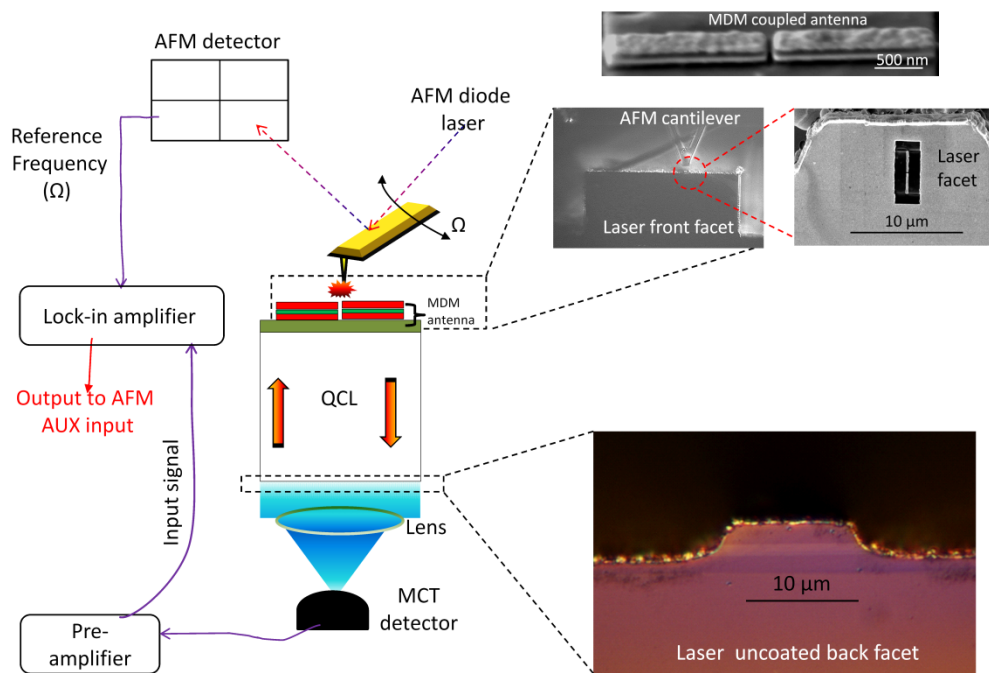
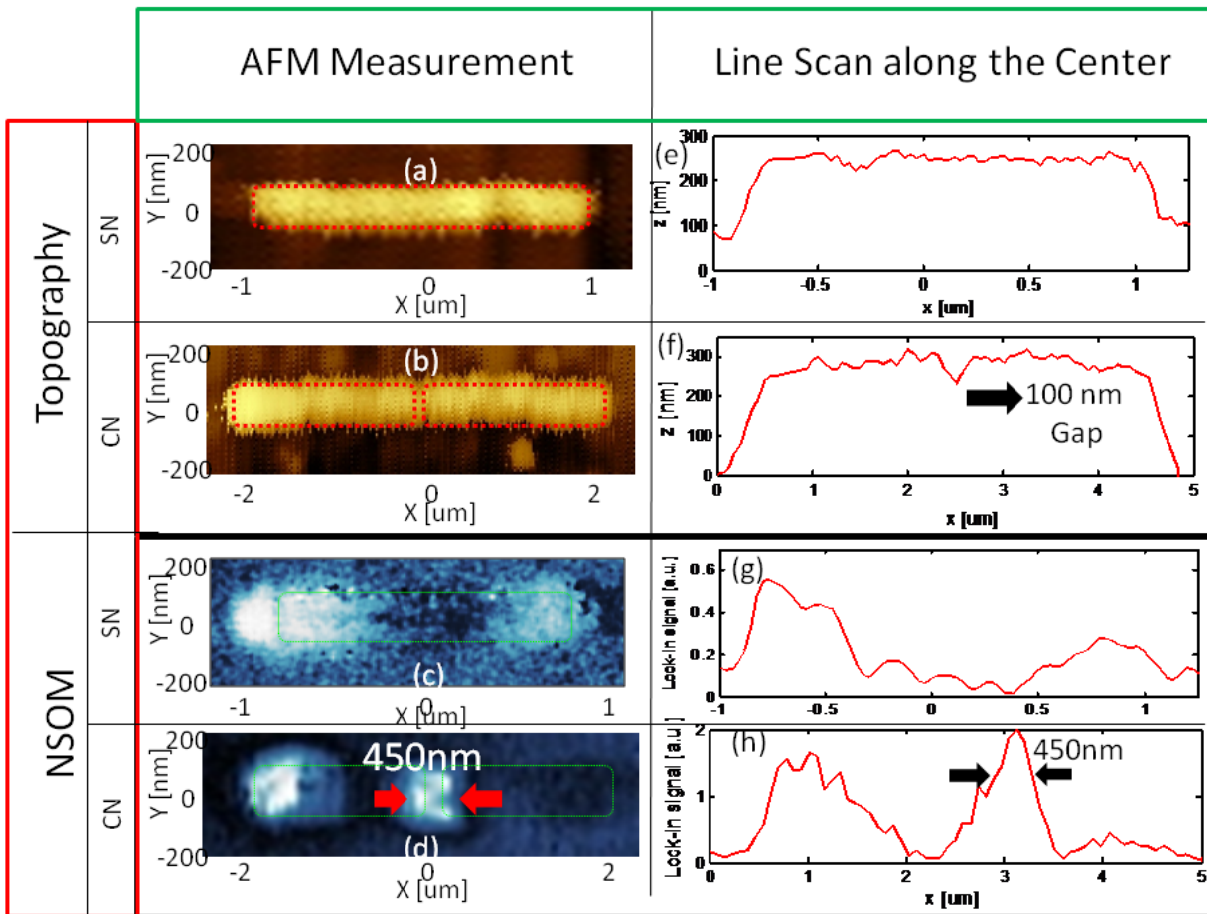


Figure 4 - Apertureless near-field optical microscope (a-NSOM) to probe near field intensity of optical antennas.

5. MEASUREMENT

Experimentally, nanorod on the laser facet was located using AFM scanning. Under laser in operation, the AFM tip-scattered near-field response is recorded simultaneously with the topography. When in plane incident field interacts with the MDM nanorod, conduction electrons in the metal respond with generating a surface Plasmon wave. For composite material based antenna surface Plasmon waves get generated at each interface between metal and dielectric.

During NSOM measurement, there are two components of scattered electric field, E_x (in-plane) and E_z (out-of-plane), interacts with the oscillating AFM probe. Unlike in phase dipole oscillation as in E_x , the E_z field components at opposite ends of the nanorod oscillate out of phase with respect to each other by a relative angle $\varphi=\pi$. We have shown the near field image of Au-SiO₂-Au (75/20/75nm) single and coupled nanorod antenna, with an antenna arm length of $L=2.0\mu\text{m}$, integrated on the facet of room temperature working QCL in Figure -5 (c)-(d). We experimentally measure the E_z instead of E_x component of the electric field. Unlike interferometric NSOM^{54,55,56}, a-NSOM can't selectively measure two different components of E-field and thus only the significant component of the near field is expected to be recorded. As been described in ref 51, the electric field component parallel to the sample surface yields a relatively weak scattering signal compared to the component perpendicular to it. It is due to difference between their effective polarizability. Thus probing out-of-plane E_z component ideally suited for such measurement. We have found a more intense spot at the left corner of the nanorod compared to the right (Figure -5(c)). Similar observation has been reported in ref 32 and it is due to unsuppressed background noise. The line scans of topography and near field are shown in Figure 5(e) – (h). The image distortions, as seen Figure-5 (a) – (b), is due to small sample drift and it is because the long acquisition time (~ 1 hour) for a-NSOM measurement.



* SN= Single nanorod ; CN= Coupled nanorod

Figure 5 - (a) –(b) Topography , (c)- (d)NSOM image of the Au-SiO₂-Au single and coupled nanorod antenna integrated on the facet of a room temperature working quantum cascade laser. The line scan along the center of each structure (a),(b), (c), (d) is shown in the right column of the above figure. The asymmetric nature of the NSOM image in figure (d) has been discussed in ref 57.

6. FUTURE WORK

To be able to investigate bio-molecules, which have vibration frequency in the mid-infrared region of optical spectrum, the detection volume must be reduced by an order of magnitude. The QCL integrated optical antenna has shown squeezing of optical spot within a small volume (radius ~ 12 times smaller than the operating wavelength). Thus any bio or chemical molecule, which has vibration resonance matching the lasing frequency, can have a strong absorption while inside the confined spot size. Now the challenge comes to develop a process to load such molecules at specific location of the antenna where the near field enhancement takes place. Further, the loading process needs precise control so that it doesn't affect reflectivity of laser front facet (directly related with lasing performance). We are on a process to develop an opto-fluidic platform to control the flow of fluid over the "hot spot" regions based on polydimethylsiloxane (PDMS) material. Low cost, rapid prototyping, reusability of the master molds, thermosetting nature and multilayer fabrication to create complex 3-dimensional systems make PDMS superior compared to other elastomeric materials available for soft lithography. Furthermore, replica molding using elastomers enables easy installation of fluidic interconnections as well as implementation of on-chip pressure driven flow through multilayer fabrication capabilities. Fluid flow through the microchannels can be controlled either by external pumps or by microfabricated components integrated on-chip. A more detailed description about this work can be found in ref⁵⁸

7. CONCLUSIONS

During the NSOM measurement, the laser was operated at 1% duty cycle near the threshold voltage with an average power output of $100\mu\text{W}$. The near-field images of the antenna were recorded with high pixel resolution and with a reduced scan speed of 0.1 line/s. The NSOM images show excellent agreement with the z-component of the simulated near field distribution (not shown in this paper). The full widths at half maximum (FWHM) of the "hot spot" were found to be $\sim 450\text{nm}$. The spot is naturally confined along the short direction of the antenna width of 100nm . The generated power flux at each hot spot is calculated as the total operating laser power divided by number of spots and spot area. Neglecting any incurred optical losses the total power flux is calculated to be approximately $0.8\text{nW}/\text{nm}^2$ per hot spot. Even at 1% of this value, there will be enough optical power to have an interaction with single molecules⁵⁹.

In conclusion, we have demonstrated near field scanning optical microscopy of a single and coupled nanorod antenna integrated on to the facet of a room temperature working QCL. The presented composite material based antenna designs can generate a very small optical spot size with power flux density in the order of nW/nm^2 . Simulations have confirmed that its multilayered design can significantly increase this intensity enhancement. Such high power densities combined with multiple hot spot location on the same antenna will enable us to detect single molecule based on their unique vibrational signature.

8. ACKNOWLEDGEMENT

This work was partially funded by NSF grant CBET-0932611. The Focused Ion beam milling and SEM studies were performed in the (EPIC) (NIFTI) (Keck-II) facility of NUANCE Center at Northwestern University. NUANCE Center is supported by NSF-NSEC, NSF-MRSEC, Keck Foundation, the State of Illinois, and Northwestern University. The Materials Research Center (MRC) cleanroom facility at Northwestern University was used for ebeam evaporation. The micro-fluidic platform is being built with collaboration with Prof. Dino Di Carlo at University of California, Los Angeles, USA.

¹ H. Raether. "Surface plasmons on smooth and rough surfaces and on gratings". (Springer, 1999)

² T.W. Ebbesen, H.J. Lezec, H. F. Ghaemi, T. Thio and P. A. Wolff. "Extraordinary optical transmission through sub-wavelength hole arrays," Nature. **391**, 667 (1998)

³ A.Lesuffleur, I. H. Im, N. C. Lindquist, S. H. Oh. "Periodic nanohole arrays with shape-enhanced Plasmon resonance as real time biosensors," Applied Physics Letter. **90**, 261104 (2007)

- ⁴ Y. Lie, J. Bishop, L. Williams, S. Blair and J. Herron. "Biosensing based upon molecular confinement in metallic nanocavities," *Nanotechnology* **15**, 1368 (2004)
- ⁵ C.T. Cambell and K.G. Him. "SPR microscopy and its applications to high-throughput analyses of biomolecular binding events and their kinetics," *Biomaterials* **28** (15), 2380-2392 (2007)
- ⁶ S. Nie and S. R. Emory. "Probing single molecule and single nanoparticles by surface enhanced raman scattering," *Science* **275**, 1102 (1997)
- ⁷ B. Liedberg, C. Nylander and I. Lunstrom. "Surface plasma resonance for gas detection and biosensing," *Sensor and Actuators* **4**, 299 (1983)
- ⁸ M.A. Cooper. "Optical bio sensors in drug discovery," *Nat. Rev. Drug Discovery* **1**, 515 (2002)
- ⁹ Z. Liu, J. M. Steele, W. Srituravanich, Y. Pikus, C. Sun and X. Zhang. *Nano Letter.* **5**, 1726 (2005)
- ¹⁰ K. Kneipp, Y. Wan, H. Kneipp, L. T. Perelman, I. Itzkan, R. Dasari and M. S. Field. "Single molecule detection using surface-enabled Raman scattering," *Physical Review Letter.* **78**, 1667 (1997)
- ¹¹ W.L. Barnes, S. C. Kitson, T. W. Priest and J.R. Sambles. "Photonic surfaces for surface Plasmon polaritons" *Journal of the optical society of America A – Optics image Science and vision.* **14**, 1654-1661 (1997)
- ¹² G. Mie. "Articles on the optical characteristics of turbid tubes, especially colloidal metal solutions," *Annalen Der Physik*, vol. **25**, 377-445 (1908)
- ¹³ R. Marty, G. baffou, A. Arbouet, C. Girad and R. Quidant. "Charge distribution inside complex plasmonic nanoparticles," *Optics Express.* Vol **18**, No 3 (2010)
- ¹⁴ T.H.Taminiau, F. D. Stefani, F. B. Segerink and N.F. van Hulst. "Optical antennas direct single-molecule emission," *Nature Photonics* **2**, 234-237 (2008)
- ¹⁵ V. Giannini and J. A. Sanchez-Gil. "Excitation and emission enhancement of single molecule fluorescence through multiple surface-plasmon resonances on metal trimer antennas," *Optics Letter* **33**, 899-901 (2008)
- ¹⁶ P. Krenz, J. Alda and G. Boreman. "Orthogonal infrared dipole antenna," *Infrared Physics Technology.* **51**, 340-343 (2008)
- ¹⁷ C. Fumeaux, M. A. Gritz, I. Codreanu, W. L. Schaich, F. J. Gonzalez and G. D. Boreman. "Measurement of the resonance lengths of infrared dipole antennas," *Infrared Physics Technology* **41**, 271-281 (2000)
- ¹⁸ N. Yu, E. Cubukcu, L. Diehl, M. A. Belkin, K. B. Crozier, F. Capasso, D. Bour, S. Corzine and G. Hofler. "Plasmonic quantum cascade laser antenna," *Applied Physics Letter* **91**, 173113 (2007)
- ¹⁹ A.Cvitkovic, N. Ocelic, J. Aizpurua, R. Guckenberger and R. Hillenbrand. "Infrared imaging of single nanoparticles via strong field enhancement in scanning nanogap," *Physical Review Letter* **97**, 060801 (2006)
- ²⁰ L. Tang, S. E. Kocabas, S. Latif, A. K. Okyay, D. S. Ly-Gagnon, K. C. Sarswat and D. A. B. Miller. "Nanometre-scale germanium photodetector enhanced by a near-infrared dipole antenna," *Nature Photonics* **2**, 226-229 (2008)
- ²¹ M. Pelton, J. Aizpurua and G. Bryant. "Metal-nanoparticle plasmonics". *Laser Photon. Rev.* **2**, 135-159 (2008)
- ²² J.N. Farahani, D. W. Pohl, H.J. Eisler and B. Hecht. "Single quantum dot coupled to a strong scanning optical antenna: A tunable super emitter". *Physical Review Letter* **95**, 017402 (2005)
- ²³ S. D. Lie, M. T. Cheng, Z. J. yang and Q. Q. Wang. "Surface plasmon propagation in a pair of metal nanowires coupled to nanosized optical emitter" *Optics Letter* **33**, 851-853 (2008)
- ²⁴ F. Neubrech, T. Kolb, R. Lovrincic, G. Fahsold, A. Pucci, J. Aizpurua, T. W. Cornelius, M. E. Toimil-Molares, R. Neumann and S. karim. "Resonances of individual metal nanowires in the infrared". *Applied Physics Letter* **89**, 253104 (2006)
- ²⁵ J. Merlein, M. Kahl, A. Zuschlag, A. Sell, A. Halm, J. Boneberg, P. Leiderer, A. Leitenstorfer and R. Bratschitsch. "Nanomechanical control of an optical antenna" *Nature Photonics* **2**, 230-233 (2008)
- ²⁶ K.B.Crozier, A. Sundaramurthy, G.S. Kino and C. F. Quante. "Optical antennas: Resonators for local field enhancement". *Journal of Applied Physics* **94**, 4632-4642 (2003)
- ²⁷ F.J.Gonzalez and G.D.Boreman. "Comparison of dipole, bowtie, spiral and log-periodic IR antennas" *Infrared Phys. Technol.* **46**, 418-428 (2005)
- ²⁸ R.D. Grober, R. J. Schoelkopf and D.E. Prober, "Optical antenna: Towards a unity efficiency near-field optical probe" *Applied Physics Letter.* **70**, 1354 (1997)
- ²⁹ E. R. Encina and E. A. Coronado. "Resonance conditions for multipole plasmon excitations in noble metal nanorods," *Journal Physical Chemistry C* **111**, 16796 (2007)
- ³⁰ J.Aizpurua, G. W. Bryant, L. J. Richter, F. J. Garcia de Abajo, B. K. Kelley and T. Mallouk. "Optical properties of coupled metallic nanorods for field-enhanced spectroscopy," *Physical Review B* **71**, 235420 (2005)

- ³¹ R. L. Olmon, P. M. Krentz, A. C. Jones, G. D. Boreman and M. B. Raschke. "Near-field imaging of optical antenna modes in the mid-infrared," *Optics Express* vol **16**, No 25 (2008)
- ³² M. Schnell, A. G. Etxarri, A. J. Huber, K. B. Crozier, A. Borisov, J. Aizpurua and R. Hillenbrand. "Amplitude and phase-resolved near field mapping of infrared antenna modes by transmission mode scattering type near field microscopy," *Journal of Physical Chemistry* Vol **114**, No 16 (2010)
- ³³ M. Rang, A. C. Jones, F. Zhou, Z. Y. Li, B. J. Wiley, Y. Xia and M. B. Raschke. "Optical near-field mapping of plasmonic nanoprisms" *Nano Letter* Vol **8**, No 10 (2008)
- ³⁴ J. Faist, F. Capasso, D. L. Sivco, C. Sirtori, A. L. Hutchinson, and A.Y. Cho. "Quantum Cascade Laser" *Science* **264**, 553 (1994)
- ³⁵ Y. Bai, S. Slivken, S. Kuboya, S. R. Darvish and M. Razeghi. "Quantum cascade laser that emits more light than heat," *Nature Photonics* **4**, 99 (2010)
- ³⁶ Y. Bai, S. Slivken, S. R. Darvish, M. Razeghi. "Room temperature continuous wave operation of quantum cascade laser with 12.5% wall-plug efficiency," *Applied Physics Letter* **93**, 021103 (2008)
- ³⁷ E. Cubukcu, E.A. Kort, K. B. Crozier and F. Capasso. "Plasmonic laser antenna," *Applied Physics Letter* **99**, 093120 (2006)
- ³⁸ N. Yu, E. Cubukcu, L. Diehl, M. A. Belkin, K. B. Crozier, F. Capasso, D. Bour, S. Corzine, G. Hofler. "Plasmonic quantum cascade laser antenna," *Applied Physics Letter* **91**, 173113 (2007)
- ³⁹ N. Yu, E. Cubukcu, L. Diehl, D. Bour, S. Corzine, J. Zhu, G. Hofler, K. B. Crozier, and F. Capasso "Bowtie plasmonic cascade laser antenna," *Optics Express* **15**, 13272 (2007)
- ⁴⁰ E. Cubukcu, N. Yu, E. J. Smythe, L. Diehl, K. B. Crozier and F. Capasso. "Plasmonic laser antenna and related devices," *IEEE Journal of Selected Topics in Quantum Electronics* **14**, 1448 (2008)
- ⁴¹ N. Yu, R. Blanchard, J. Fan, Q. J. Wang, C. Pflugl, L. Diehl, T. Edamura, M. Yamanishi, H. Kan and F. Capasso "Quantum cascade lasers with integrated plasmonic antenna-array collimator," *Optics Express* **16**, 19447 (2008)
- ⁴² N. Yu, R. Blanchard, J. Fan, Q. J. Wang, C. Pflugl, L. Diehl, T. Edamura, S. Furuta, M. Yamanishi, H. Kan and F. Capasso. "Plasmonics for laser beam shaping," *IEEE Transactions on Nanotechnology* **9**, 11 (2010)
- ⁴³ K. H. Su, Q. H. Wei and X. Zhang. "Tunable and augmented Plasmon resonances of Au/SiO₂/Au nanodisks," *Applied Physics Letter* **88**, 063118 (2006)
- ⁴⁴ A. Dmitriev, T. Pakizeh, M. Kall and D. S. Sutherland. "Gold-Silica-Gold nanosandwiches " Tunable Biomodal Plasmonic Resonators," *Small* Vol **3**, 294-299 (2007)
- ⁴⁵ K. H. Su, S. Durant, J. M. Steele, Y. Xiong, C. Sun and X. Zhang. "Raman enhancement factor of single tunable nanoplasmonics resonator," *Phys. Chem. B* **110**, 3964 (2006)
- ⁴⁶ E. D. Palik. "Handbook of Optical constants of solids". (Academic Press, New York, 1985)
- ⁴⁷ D. Dey, J. Kohoutek, R. M. Gelfand, A. Bonakar and H. Mohseni. "Composite nano-antenna integrated with quantum cascade laser" *IEEE Photonics Technology Letters* **22**, 32 (2010)
- ⁴⁸ D. Dey, J. Kohoutek, R. M. Gelfand, A. Bonakar and H. Mohseni. "Metal-dielectric-metal nano antenna integrated with quantum cascade laser" *Optics Letter* **35**, 2783 (2010)
- ⁴⁹ J. Kohoutek, D. Dey, R. M. Gelfand, A. Bonakar and H. Mohseni. "An apertureless near-field scanning optical microscope for imaging surface plasmon in the mid-infrared" *Proc. SPIE* **7787**, 77870R-1 (2010)
- ⁵⁰ B. Knoll and F. Keilmann. "Enhanced dielectric contrast in scattering-type scanning near-field optical microscopy". *Optics Communication* **182**, 321 (2000)
- ⁵¹ R. Hillenbrand, B. Knoll and F. Keilmann. "Pure optical contrast in scattering-type scanning near-field microscopy," *Journal of Microscopy* **202**, 77-83 (2000)
- ⁵² H. C. Liu. "Intersubband transition in Quantum wells: Physics and device application II" Academic Press (1999)
- ⁵³ R. Rang, A. C. Jones, F. Zhou, Z. Li, B. J. Wiley, Y. Xia and M. B. Raschke. "Optical Near-field mapping of plasmonic nanoprisms," *Nano Letter* **8**, 3357-3363 (2008)
- ⁵⁴ M. Schnell, A. Garcia-Etxarri, A. J. Huber, K. Crozier, J. Aizpurua and R. Hillenbrand. "Controlling the near-field oscillations of loaded plasmonic nanoantennas," *Nature Photonics* **3**, 287 (2009)
- ⁵⁵ J. Dorfmueller, R. Vogelgesang, R. T. Weitz, C. Rockstuhl, C. Etrich, T. Pertsch, F. Lederer and K. Kern. "Fabry-perot resonance in one-dimensional plasmonic nanostructures," *Nano Letter* **9**, 2372 (2009)
- ⁵⁶ R. L. Olmon, P. M. Krenz, A. C. Jones, G. D. Boreman and M. B. Raschke. "Near-field imaging of optical antenna modes in the mid-infrared," *Optics Express* **16**, 25 (2008)
- ⁵⁷ D. Dey, J. Kohoutek, R. M. Gelfand, A. Bonakar and H. Mohseni. "Plasmonic antenna integrated on the facet of quantum cascade laser for chip-scale molecular sensing" *IEEE Sensor Conference* pp.454-458 (2010)

- ⁵⁸ R. M. Gelfand, D. Dey, J. Kohoutek, A. Bonakder, S.C. Hur, D. Di Carlo and H. Mohseni. "Towards an integrated chip-scale Bio sensor" *OPN Optics and Photonics News* **22**, 32 (2011)
- ⁵⁹ M. F. Garcia-Parajo. "Optical antenna focusing in on biology," *Nature*, **2**, 201 (2008)